Cellulose fiber-reinforced composites—History of evolution, chemistry, and structure

1

Aditya Kataria[a], *Swati Chaturvedi*[a], *Vaibhav Chaudhary*[a], *Akarsh Verma*[a,b], *Naman Jain*[c], *Mavinkere Rangappa Sanjay*[d], *and Suchart Siengchin*[d]
[a]Department of Mechanical Engineering, University of Petroleum and Energy Studies, Dehradun, Uttarakhand, India, [b]Brigham Young University, Provo, UT, United States, [c]Department of Mechanical Engineering, ABES Engineering College, Ghaziabad, India, [d]Department of Materials and Production Engineering, The Sirindhorn International Thai–German Graduate School of Engineering (TGGS), King Mongkut's University of Technology North Bangkok, Bangkok, Thailand

1.1 Introduction

The increment in natural consciousness and local area interest, the new natural guidelines, and unjustifiable utilization of petroleum impelled thinking about the employment of the materials that are harmless to the ecosystem. Natural cellulose fiber is thought about one of the harmless to the ecosystem materials, which have great properties contrasted with synthetic or engineered fiber (May-Pat, Valadez-González, & Herrera-Franco, 2013). Through the latest survey of 2010, it is found that the world-wide natural cellulose fiber-reinforced composites industry sector reached 2.1 billion dollars. By analyzing it and the current scenario where the use of natural & biodegradable fiber is increasing, we can assume that production and the usage of natural cellulose-reinforced composites industries is estimated to grow by 15%–20% worldwide (Uddin, Abro, Purdue, & Vaidya, 2013). Cellulose fibers are fibers made with ethers or esters of cellulose, which can be attained from the bark, wood, or leaves of plants, or other plant-based material. In addition to cellulose, the fibers may also comprise of hemicellulose and lignin, with varying percentages of these components fluctuating the mechanical properties of the fibers. Cellulose was found in 1838 by a French physicist named Anselme Payen, who segregated it from plant stock and chose its engineered formula (TheFreeDictionary.com, n.d.). Cellulose was used to convey the essential viable thermoplastic polymer, celluloid, in Hyatt Manufacturing Company in 1870. Manufacture of rayon ("fake silk") from cellulose commenced during the 1890s, and cellophane was composed in 1912. In 1893, Arthur D. Little made one more cellulosic thing, acidic corrosive determination, and made it into a film. The primary business material usages for acidic corrosive inference in fiber structure were made by the Celanese Company in the early 1920s. A scientist named Hermann Staudinger took the polymer development of cellulose in 1920. The compound was initially misleadingly linked short of the use of

Cellulose Fibre Reinforced Composites. https://doi.org/10.1016/B978-0-323-90125-3.00012-4

any naturally decided proteins in 1992, by Kobayashi and Shoda (Gilbert & Kadla, 1998). It is defined as the fibers that are not synthetic or manmade but are sourced from plants or animals. The use of natural cellulose fiber from various resources, renewable and non-renewable like bamboo, sugarcane bagasse, hemp, flax, jute, and so on to make composite materials have gained quiet a lot of consideration in the latter decades, so far. The plants that yield or give us the cellulose fiber are classified in various categories and that can be seen in Fig. 1.1.

1.2 Cellulose fiber-reinforced composites—History of evolution

Composite materials are being used for centuries. The composite term from the beginning was utilized in 1500 BC. Early Mesopotamian and Egyptian designers and craftsmen made robust and tough constructions by means of a mix of straw and mud. Since then, after 25 BC, 10 books on Architecture described the strong development and portrayed several sorts of lime and mortars. From the bygone era outline, engineers, producers, craftsman, and creators were endeavored to advance the use of composite materials in a particular field in a more refined way. In 1200 AD, Mongols arranged the essential composite bows which were crafted up of a mix of bamboo, wood, horns, cow's tendons, and silk invigorated by ordinary pine sap which was by and large staggering and utmost definite weapons until the 14th century. From here on out, from 1870 to 1890, the headway of the composite material started to vary due to the engineered distress. In the modern period, the progression of the composites materials was not underway until scientists were focused on the improvement of plastics.

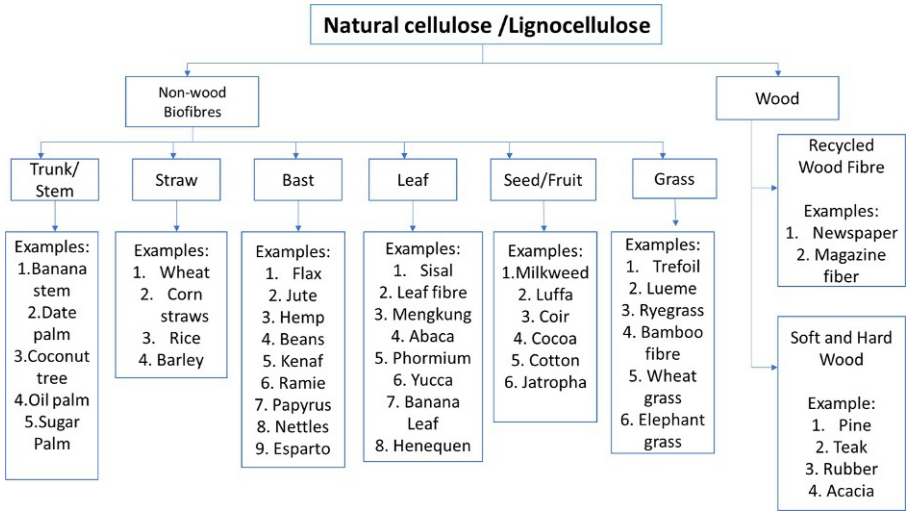

Fig. 1.1 Classification of different types of natural cellulose fiber.

During the 1900s, plastics materials like vinyl, phenolic, polystyrene, and polyester were completed and advanced. In 1907, the foremost plastics like Bakelite were developed with produced fragments. These newly designed materials were given favored execution over various composites materials. Regardless, for essential applications, plastic alone couldn't invigorate adequate and unyielding nature. In this way, for the enhancement of the strength and toughness of the plan, it was given sincere and notable help. In 1935, Owens Corning at first revealed the primary glass fiber. The improvement of tars was on track from the 1930s, taking everything into account which procedures/techniques are used in the composites business today. The blend of a plastic polymer and fiberglass made a remarkable development. Unsaturated polyester tars were authorized in 1936. Other better tar structures were beginning to see use from 1938 (Keya et al., 2019; May-Pat et al., 2013; Mohammed, Ansari, Pua, Jawaid, & Islam, 2015; Uddin, 2013).

Currently, people have started to depend upon composite materials and they do start to employ composite materials at different points. Natural cellulose fiber composite materials are eco-obliging, strong, lightweight, endless, unassuming, ecological, and viable. Natural cellulose fibers have incredible assets separating them from designed/synthetic fiber (Keya et al., 2019). Lately, basic fibers consumed as an elective help in polymer composites which have obtained thought amid various inspectors and experts because of their benefits over standard fabricated materials (Taj, Munawar, & Khan, 2007). These typical strands link jute, hemp, kenaf, coir, banana, bamboo, sugarcane, and various others (Faruk, Bledzki, Fink, & Sain, 2012), which give extraordinary mechanical properties that appeared differently with man-made strands and their cost are realistic, they are environmental and supportable, declining energy use, not as much of prosperity peril and doesn't increase wear on the equipment, not detrimental to the skin (Nguong, Lee, & Sujan, 2013). Hence, it can be utilized as a developed material because of its thermosetting and thermoplastic behavior. Thermosetting pitches like unsaturated polyester sap, polyester, epoxy, polyurethane, and phenolic are normally used for collecting composites material gives superiority in various applications. They give adequate mechanical properties and their expense is reasonable. Taking into account their incredible properties like high strength, small thickness, also, natural advantages over customary composites, regular fibers are standing apart enough to be seen among academicians, subject matter experts, and understudies and besides in industry. Because of their nondisease causing and biodegradable, the use of cellulose fiber-reinforced composites is growing step by step and quite rapidly. Natural cellulose fiber-reinforced composites are a very cost-effective material which is the reason of its use in different sectors such as aerospace, automobile, building, packaging and construction sectors, railway coach interiors, and storage devices and also acts as a replacement of high-cost glass fiber (Akil et al., 2011; Zini & Scandola, 2011).

Braga and Magalhaes (2015) considered the mechanical and thermal properties of polyester hybrid composites (e.g., jute also, glass fiber) and thought about and dissected their properties (e.g., flexural, thermal, thickness, and effect properties). He clarified that jute fiber-based composites exhibited a preferred/better conformation over glass fiber. Thwe and Liao (2000) contemplated the mechanical properties of

bamboo fiber and built up the base composite, the impact of bamboo fiber length, fiber content, bamboo to glass fiber proportion and demonstrate the mechanical properties of bamboo glass fiber-reinforced plastics. Okubo, Fujii, and Yamamoto (2004) grown new composite material utilizing bamboo fiber and polypropylene and examined the mechanical conduct of those composites. Balaji, Karthikeyan, and Sundar (2014–2015) examined the use and eventual fate of normal strands and biocomposite material and talked about their uses that can be utilized in creation of modern items because of its eco-friendly nature, minimal effort, effectively accessible conduct. Normal fiber and biocomposites are utilized to make family furniture, fencing, flooring, athletic gear, lightweight auto parts.

1.3 Chemistry

1.3.1 Glucose monomer

Cellulose is formed from a monomer called glucose. This formation takes place through condensation polymerization or can take place through biological catalysts: the enzymes through step-growth mechanisms (Shanks, 2014). Cellulose has monomer of which are very complex. Chiral carbons groups are arranged in a ring of six, which leads to a very precise stereochemistry. Monomers which have primary covalent bond needs to be developed to understand the complex nature of cellulose. This understanding also helps us in analyzing the role played by stereochemistry and interaction within and outside the molecule. Apart from four chiral, due to the linkages which are present in the chain and cyclic nature, a fifth chiral carbon arises. As a result, conformation is maintained. Cellulose is made up of repeating units of alpha 1–4 linkages between D-glucose units. Glucose is a sugar consisting of six carbons. Sixteen configurations arise due to the presence of chiral carbon (2,3,4,5). These configurations consist of both diastereoisomers and enantiomers. Glucose has a pyronase form that arises when 5-hydroxy is combined with aldehyde. As a result, the formation of six-member cyclic hemiacetal will take. There is no planarity in the cycle structure. However, in the case of glucose, the cycle structure is planar. A total of 32 diastereoisomers and enantiomers are formed due to the presence of a new chiral center in the hemiacetal hydroxyl on carbon 1. This type of conformation is called beta-glucopyranoside and is found with cellulose. Bent link is formed in starch due to the alpha-glucopyranoside which is the opposite conformation. Chirality in carbon 1 is the main reason for the difference between cellulose and starch. The stability of alpha-anomer is two times more than the stability beta-anomer. However, alpha-hydroxy is less stable. This is due to the anomeric effect. The anomeric effect takes place with the help of dipole's interaction by the electrons that are no bonded which are present on the adjacent hemiacetal-ring oxygen that is aligned with the hemiacetal hydroxy Group. The close packaging and crystal formation is ensured by the planar structure of cellulose. Loose coils formation takes place because of the bent conformation of starch. These crystallize with a complex molecule. In glucopyranoside structure, each carbon consists of hydrogen and pendant hydroxy. The hydrogen

atoms are small and are less crowded that's why they are directed out of the cyclic plane. Groups that are present out of the plane are known as axial. On the other hand, groups that are present inside the plane are called equatorial. Cellulose consists of hydroxyl groups that behave similarly to alcohol functional groups.

These hydroxyl groups react with strong bases like sodium hydroxide to form salt. The concentration of salt formed is very less because the hydroxyl groups are acidic only to a limited extent. Swelling, dyeing, and partial dissolving are done by taking advantage of the acidic behavior of hydroxyls present in cellulose. Aldehyde and carboxylic acid are formed by the oxidation of glucose at the C6 hydroxyl. Aldehydes are oxidized at carbon 1 which is in the open-chain structure to form glycolic acid. Glutamic acid is formed by the oxidation of C1 and C6 in open-chain form.

1.3.2 Glucose biopolymerization

Cellulose is formed by the biopolymerization of glucose. As a result, a regular polymer is created in which inversion of glucose which is adjacent takes place, without any change in stereochemistry. Two glucose units are present in the repeating unit of the cellulose chain. Glucose units are linked with chains of cellulose by polymerization leading to the formation of cellulose I crystal morphology. Glucose, cellobiose, and short glucans are formed by the enzymatic hydrolysis of cellulose. Complete hydrolysis leads to the formation of glucose. Multistep synthetic process is required for cellulose microfibrils. Assembly from the synthesizing sites is required for the microfibrils to be assembled from cellulose chains. This is a spontaneous process. Typically formation of crystalline cellulose type 1 takes place from biosynthesis, whole sometimes crystalline cellulose type 2 can also be formed. Synthesis of cellulose takes some place within the membrane of enzyme complexes. A complex network of microfibrils is formed through the synthesis mechanism. Polymerization of beta (1–4)-glucopyranose is done by cellulose synthase from uracil diphosphate-glucose (Guerriero, Fugelstad, & Bulone, 2010). The morphology, width of cellulose fibril deposition and extracellular chain assembly are controlled by the arrangement of cellulose synthase units (Ross, Mayer, & Benziman, 1991).

1.3.3 Cellulose structure

Cellulose has 300–1000 glucose units in each molecule and biopolymerization takes place with a high degree of polymerization. Thus, the molar mass varies from 540,000 to 1,800,000 g/mol. Therefore, it has a high molar mass and can form hydrogen bonds. The proximity of hydroxyl groups and alignment of hydroxyl groups and monomer units is determined by the orientation of hydroxyl groups within each glucose unit. Due to the regularity and symmetry of individual chains, the formation of assemblies of cellulose chains takes place which is confined to a fixed conformation by intramolecular bonding. Cellulose I crystals are less stable thermodynamically. However, it is found in abundance (Fidale, Ruiz, Heinze, & Seoud, 2008). Cellulose type II crystals were not found in abundance in plants. Ironic liquids and other components are used for determining the transition of crystal structure as a function of permeation (Cheng et al., 2011).

1.3.4 Chemical and solubility properties of cellulose

Acetal groups which link the cellulose monomers are resistant to alkali. Shorter chain length and glucose are formed when hydrolysis of cellulose takes place by hydrochloric A day sulfuric acid. In amorphous and crystallites which are less perfect and small, the rate of hydrolysis is more. Selective hydrolysis uses differential hydrolysis for the preparation of nanofibers and nanocrystals. Cellulose is oxidized by alkali when oxidizing agents are present. C6 hydroxyl is the site for oxidation, resulting in the formation of carboxylic acid. Thermogravimetry is used for studying thermal degradation. Degradation steps were revealed due to the presence of pectin, hemicellulose, and cellulose when thermal degradation of hemp was investigated. When noncellulose substances were treated with sodium hydroxide, TGA derivative peaks decreased. On the other hand, the onset temperature decreased when treated with sodium hydroxide (Rachini, Le Troedec, Peyratout, & Smith, 2009).

During the development of cotton fiber, to study the structural changes, TGA was used. There were differences noted in the primary and secondary cell walls (Abidi, Cabrales, & Hequet, 2010). Differential scanning calorimetry was utilized to sisal degradation. Nitrogen and air were used to examine raw and defatted fibers and their chemical constituents. Degradation of raw sisal took place at a higher temperature than cellulose. The reason behind this was the lignin content of the sisal (Martin, Martins, da Silva, & Mattoso, 2010).

In liquid such as water (which are organic), swelling of cellulose takes place. Sixteen aprotic solvents were used to study swelling in native and microcrystalline cotton. There are various factors on which the swelling depends such as—basicity, polarizability, molar volume, and nature of chain whether they are parallel or nonparallel (Fidale et al., 2008). In liquids and solutions, which have hydrogen bonding, cellulose is soluble. Lower critical solution temperature (LCST) phenomena are observed in cellulose. The swelling of cellulose is caused by sodium hydroxide and crystal II is formed from crystal I by mercerization process upon heating. Adding urea to sodium hydroxide increased the solubility because of the increase in hydrogen bonding. Effective solvents when lithium chloride is added for cellulose are *N*,*N*-dimethylacetamide (DMAc), *N*,*N*-dimethylformamide (DMF), and dimethylsulfoxide (DMSO), which are dipolar aprotic in nature. NMMO 9 (*N*-methylmorpholine-*N*-oxide) exists in solid form at room temperature, that's why solutions are made at a higher temperature. It is used to dissolve cellulose and purification. It is nonvolatile in nature and can precipitate cellulose, after dilution with water. It can then recycle after the evaporation of water from the NMMO filtrate. Cellulose fibers are regenerated under the names Lyocell, Tencel, from NMMO solutions, by injecting them into a precipitation bath.

1.3.5 Sources of cellulose

The cell wall and structural component of plants consist of cellulose. Fabrics of the fungi cell walls, insects, mollusks, and the exoskeleton of crawfishes are made up of polysaccharides and chitin. Cellulose, lignin, pectin, and hemicellulose constitute the composite of the plant cell wall which provide rigidity and strength and helps in preventing

swelling of the cell. Wood is the main source of cellulose. About 30%–40% of cellulose is present in wood and the composition also depends on the species of wood.

1.3.6 Separation of cellulose

Many other plant components along with cellulose fibers co-exist which are necessary for the functioning of the plant but they play no role in mechanical properties and performance. Adhesion of fibers with a polymer matrix causes these components to detract. These components can lose their color when comes in contact with heat or sunlight. Retting is a selective natural purification step in which the plant material is left in contact with stagnant water. It helps in further purification as the original plant material gets degraded. Decortication is a process where materials of plants are physically beaten; this is done by passing them through rollers. Since they are flexible and stronger than the rest of the plant; therefore, these fibers resist mechanical rupture.

Physical disruption of fibers takes place with the steam explosion. Heating the fibers under pressure increases the temperature of water above atmospheric boiling temperature. Water boils because of the sudden release of pressure. Physical disruption is caused because of the force of the boiling water. Due to the properties such as strength, crystal structure, and limited water uptake as compared to the rest of the material, no significant damage takes place in these fibers. The formation of 5-hydroxymethylfurfural is a sign of cellulose degradation (Jacquet et al., 2011).

1.3.7 Purification of cellulose

Organic solvent extraction with acetone or ethanol, to remove waxes is generally the first step in the purification of cellulose. The absorptivity of water in fibers increases after alkali extraction. After that, extraction of alkali is used for dissolving lignin and pectins. Phenolic groups are present in lignins and carboxyl groups are present in pectins and hemicellulose (Shanks, 2014). During alkali treatment, swelling of cellulose takes place. Chemical procedures such as acid hydrolysis, chlorination, alkaline extraction are used for the purification of cellulose (Astley & Donald, 2001; Morán, Alvarez, Cyras, & Vázquez, 2008). In amorphous regions, the rate of acid hydrolysis is more. As a result, the cellulose which is left after a major portion of cellulose is pure.

For bleaching the product of cellulose, oxidative alkaline extraction is used. This treatment produces carboxyl groups that are soluble in the alkali of sodium hypochlorite and chlorite. When enzyme pectinase is used, a milder and selective form of hydrolysis is used. *Aspergillus aculeatus* is used for preparing pectinase. Pectin which is the component of the cell wall hydrolyses pectinase. In the pH buffer, a pectinase solution is used to incubate raw cellulose.

1.3.8 Cellulose polymorphism

Depending on the source and treatment, crystalline cellulose can take several morphologies. Cellulose type I is known as native cellulose. It is mostly found in cell walls and other plant structures. On the other hand, cellulose type II is known as textile

cellulose. It is mostly obtained by a process called mercerization in which strong alkalis are heated. Cellulose III and cellulose IV are mostly found in combination with types I and II. Cellulose I has unit cell lattice parameters of $a = 0.835$ nm; $b = 1.03$ nm; $c = 0.79$ nm and crystallizes in monoclinic form.

Crystal size from equatorial reflection and apparent crystal length from meridional reflections were obtained when diffraction peak widths were analyzed. To characterize crystal dimensions and shape, small-angle X-ray scattering was used. To measure the cellulose fibril structure, SAXS (small-angle X-ray scattering) was performed on flax fibers. Hydration level was responsible for microfibril misalignment. Repeat distance of about 0.6–0.7 was found in crystalline and noncrystalline. In dry and wet states, structures of fibers differed (Vorawongsagul, Pratumpong, & Pechyen, 2021). SAXS (small-angle X-ray scattering) and WAXS were used to measure fiber symmetry of collagen and cellulose. Fibers exhibit cylindrical rotational symmetry, thus WAXS can be used to determine the oriental angle.

1.3.9 Chemical modification of cellulose

Solubility is imparted by alkyl cellulose such as methyl and ethyl cellulose by varying their amount used for substitution. Methylcellulose is soluble in water and can behave as a rheological agent when the degree of substitution is low. Methylcellulose becomes soluble in organic solvents with higher substitutions. Transient Rheological and Isotropic liquid crystalline solution behavior is noticed when ethyl cellulose solutions are placed in m-cresol. The free hydroxyl group can be reduced by using and the combinations that can be formed from these derivatives.

1.3.10 Preparation of nanocellulose

There are various structures of cellulose example—MCC, bacterial cellulose, CNF, CNC where dimensions are small and internal structure is maintained. When purified cellulose is hydrolyzed by partial and selective method, formation of each form takes place. After mixing aqueous mineral acid with cellulose, suspension formation takes place which is diluted. Amorphous and semicrystal are hydrolyzed first, thus having the most perfect crystal structures.

1.4 Structures

1.4.1 Cellulose reinforcement in polylactic acid and polybutylene succinate

This study was aimed at making cellulose fiber-reinforced PLA/PBS with the help of a twin-screw extruder along with injection molding (Vorawongsagul et al., 2021). Its mechanical properties of the structures were investigated and reported.

1.4.1.1 Melt flow index of the composite

The index melt flow is used to quantify the viscosity of the melt which shows that a lower melt flow rate is linked to higher melt viscosity. The addition of cellulose fibers in the PLA/PBS blend led to a growth in the melt flow index and subsequently, a reduction in the viscosity of PLA/PBS/CF with respect to pure PLA or PBS. In a low-frequency range, a substantial increase in the intricate viscosity of composites occurred. Because the fibers were oriented in the flow direction, all composites exhibited shear thinning. At a phr value of 15 for the loading of CF, the highest filling effect was obtained. Bhatia, Gupta, Bhattacharya, and Choi (2007) reported that lesser content of cellulose fibers in the PLA/PBS matrix had established itself due to higher viscosity of the melt in the entire array of the shear rates present. The value of the melt flow index diminished when the amount of CF taken was escalated from a value of 5 phr to 15 phr, but also increased the probability of distribution of fiber in the matrix. Hence, the ideal value is kept at 15 phr for the appendage of CF in PLA/PBS.

Meant for the production of foam, foam injection molding through chemical foaming is used. The chemical foaming agent can be added in two ways, first through the hopper of the injection molding machine along with the polymer pellets, and second when plasticization of the polymer is ongoing in the barrel. The foaming agent dissolves throughout the procedure. During foam extrusion, the spin of the screw pushes out the melt forwards and exits out of the extruder die. In foam injection molding, the screw revolves and simultaneously moves rearward because of the gathering of a pool made up of a gas-polymer mix by the screw's end. The extreme pressure and temperature in the unit where plasticization occurs, deliver a supercritical condition of the foaming agent during the chemical foaming procedure. To attain a high degree of solubility, CO_2 is used as a chemical foaming agent and utilized in an overcritical state. Since a fluid has a low viscosity, high diffusion properties, and low surface tension, providing it brilliant solubility in the polymer (Mathew, Oksman, & Sain, 2005; Yu et al., 2015).

1.4.1.2 SEM analysis of composite foams

SEM analysis is done to find the shape and size of the cellulose fibers and their compatibility with the polymer matrix. The standard thickness of the CF was around $16.19 \pm 0.33\,\mu m$. Vorawongsagul et al. (Astley & Donald, 2001) reported that the cell wall structures of PLA/PBS and PLA/PBS-CF foams show closed-cell walls due to sodium bicarbonate decomposing into carbon dioxide gas that facilitates sealed cells on biofoam structures. Melt-based foam construction machineries were combined with other means to increase porosity. To generate pores, various methods like foaming of gas and phase separation methods were used. The composite foam consisting of CF was larger than PLA/PBS foam by 5 phr. When the content of CF was improved, the quantity of cells and uniformity of distribution of cells also increased. Cellulose fibers were helpful in the improvement of the properties of gas barriers. The polymer's viscosity decides the bubble growth bubbling shape (Ma et al., 2012). The best foam was with a CF content of 15 phr, i.e., PLA/PBS-CF15

as it was the most uniform in terms of shape and cell size. The number of closed cells was also increased when the PLA/PBS foam was dipped in hot water for 75°C for 30 min. Increasing the temperature expands the material and increases the diffusivity. Sodium bicarbonate has two states, one exists at 80°C, which leaves solid sodium bicarbonate, and second at 120–150°C, which leaves solid sodium oxide (Sadik, Pillon, Carrot, & Ruiz, 2018).

1.4.1.3 FTIR spectroscopy

The adsorption peaks of PLA foam were observed at 3299 cm^{-1} for C-H vibrations and at 1749 cm^{-1} for CO═ vibrations. In PBS foam, —OH vibrations was observed at 3300 cm^{-1}, CO═ vibrations at 1712 cm^{-1}, CO— vibrations at 1155 cm^{-1}, and C-H vibrations at 2919 cm^{-1} (Cai, Lv, & Feng, 2013). The peak of CF was observed at 3333 cm^{-1} for —OH vibrations, at 2897 cm^{-1} for C-H vibrations, and 1031 cm^{-1} for CO— vibrations. No new peaks were observed in the PLA/PBS-CF composite.

1.4.1.4 XRD analysis

The diffraction peaks of PBS foam were observed, recorded as (020) at $2\theta = 19.5°$ and (110) at $2\theta = 22.5°$ of a crystalline of monoclinic nature (Wang et al., 2013). For PLA foam, a broad peak was observed, which can be attributed to a small level of matrix crystallinity due to quick cooling rates when the foam underwent extrusion and injection molding. The fibers exhibited strong peaks at $2\theta = 15.8°$ and 22.6° with index to (200) and (002) (Mathew et al., 2005; Zhao et al., 2007). PLA/PBS blends don't show any strong peaks in the XRD pattern. The XRD of PLA/PBS-CF composite foams exhibiting a peak at $2\theta = 16.6°$ and 22.6° as the most protuberant and telling of CF crystallinity. As CF matter is increased to 15 phr, a stable increment in the concentration of the peak at $2\theta = 16.6°$ and 22.6° is detected, which were not projecting at low reinforcement content. Hence, it was observed that 15 phr of fibers has a higher-level crystallinity of the matrix than when CF is not added, which can also explain the lower tensile modulus of the PLA/PBS when compared with PLA/PBS-CF.

1.4.1.5 Mechanical properties

The accumulation of cellulose fibers to the PLA/PBA foam increased its mechanical properties both when it was immersed in hot water, and when it was not submerged in hot water. When the CF content was increased from 0 to 15 phr, an increase in tensile strength from 36.51 MPa at 0 phr to 42.30 MPa at 15 phr was observed. The Young's modulus also increased from 1146.57 MPa at 0 phr to 1393 MPa at 15 phr. This exhibits that an increase in the CF content will proportionally increase the modulus value (Mulinari & Da Silva, 2008). For the complete values, refer to Table 6 in the reference (Vorawongsagul et al., 2021). Due to the addition of CF fibers, the rigidity of the composite increased, which resulted in the decrease of elongation percentage upon addition of stress (Mulinari, Voorwald, Cioffi, & da Silva, 2017). Conversely, an increase in the elongation was observed upon growing the CF content. Upon

immersion in boiling water, the tensile strength of the composite foams with CF was reduced because the superior the closed-cell of composite foams, the lower the density.

1.4.2 Cellulose reinforcement in natural bamboo-composite

This study was aimed at removing cellulose fibers from bamboo stalks and using them as reinforcement for an epoxy composite (Kalali, Hu, Wang, Song, & Xing, 2019). The mechanical properties of the composite include ultimate tensile strength, specific tensile strength, modulus, and impact strength. Characteristic analyses like SEM and FTIR were also reported. These tests were then compared with other materials like normal epoxy, TRIPLEX, and Al alloy 2000 to benchmark the composite prepared.

1.4.2.1 FTIR analysis

The lignin present in the bamboo was first removed, and then FTIR was done to confirm its removal. To do so, the analysis was done on both natural bamboo and the lignin removed bamboo. Natural bamboo exhibited many characteristic lignin bands along with bands at 1735 cm^{-1} for carbonyl vibrations (Sánchez, Aperador, & Capote, 2018), 1602, 1510, 1421, and 1327 cm^{-1} for aromatic skeletal (Zhang et al., 2017, 2018), 1460 cm^{-1} C-H vibrations due to —OCH_3 (Nishida, Tanaka, Miki, Ito, & Kanayama, 2017), and at 1167 cm^{-1} due to carbonyl vibration (Zhang et al., 2017). When this analysis was done on the de-lignified bamboo, the lignin bands were missing, exhibiting the successful removal of lignin from the bamboo stalks. A reduction in the density between bulk bamboo and de-lignified bamboo also verified the same fact. Delignified bamboo had a bulk of 0.26 g/cm^3, while the loose bamboo had a bulk of 0.60 g/cm^3.

1.4.2.2 SEM analysis

SEM images of the natural bamboo in the upright direction to growth displayed a porous structure made up of fiber bundles, parenchyma cells, and vessels, while the same images in the growth direction showed the fibers bound by lignin. Removal of lignin led to a honeycomb structure. Additionally, the microstructure along well-aligned fibers along the growth direction was well-maintained during the chemical treatment procedure to remove lignin. Epoxy resin was then permeated into the de-lignified bamboo microstructures under the assistance of vacuum. The analysis also showed that each and every one the gaps and channels were entirely occupied with the epoxy resin. The distinction between the original bamboo cell walls and the epoxy resin is clear, signifying that the crude bamboo microstructures were also well conserved after the epoxy penetration procedure. In the direction of growth, due to the presence of epoxy resin, the surface of the fiber packs had become coarser and the fibers were associated to each other, which were expected to form a sturdy bond between the infiltrated epoxy resins and bamboo cellulose fibers.

1.4.2.3 Mechanical properties

The removal of lignin and penetration of epoxy caused in the epoxy permeated bamboo-composite helped in meaningfully improving the strength. The ultimate tensile strength of natural bamboo was 68.55 MPa. In comparison to crude bamboo, the ultimate tensile strength of the lignin removed bamboo was reduced to 36.64 MPa, due to the fact that the lignin served as a supporting binder in the cellulose fibers was uninvolved. On the other hand, the epoxy-filled bamboo-composite showed an ultimate tensile strength of 162.12 MPa, twice the values for crude bamboo. The ultimate tensile strength for the epoxy infiltrated bamboo composite is more appreciable than the previously reported values, such as 28.1 MPa for small bamboo fiber-reinforced epoxy composite (Yu, Huang, & Yu, 2014), 32.05 MPa for bamboo epoxy composite (Khan, Yousif, & Islam, 2017), 79.11–99.62 MPa for bamboo-epoxy composites preserved with different silanes (Kushwaha & Kumar, 2010), 89 MPa for bamboo fibers/bio-based epoxy modified by means of starch nanocrystal and 88 MPa silica fume which is silanized (Gauvin, Richard, & Robert, 2018), and 80.24–133.39 MPa for bamboo stripped fiber-reinforced epoxy composites (Costa, Monteiro, & Loiola, 2011). Also, the lightness of the bamboo fibers lead to high specific strength of the epoxy infiltrated bamboo composite with a value of 145 MPa cm^3/g, which was much extreme than an epoxy matrix at about 72 MPa cm^3/g (Yang, Wu, Guan, Shao, & Ritchie, 2017) and became comparable to the light-weight TRIPLEX steels which exhibited a value of 157 MPa cm^3/g and aluminum alloy which was around 167 MPa cm^3/g (Dursun & Soutis, 2014; Frommeyer & Brüx, 2006).

Moreover, the epoxy infiltrated bamboo-composite displayed an improvement of 63% in its modulus, when associated with natural or crude bamboo. As reported by Ritchie (2011), explaining the struggles between strength and toughness in materials is an ongoing and challenging task, since these tend to be reciprocally exclusive. The composite also had a sophisticated strain at 3.5% when compared to the natural bamboo which was at 1.6%. Additionally, for the characterization of the ductility of the samples, the Izod impact test was conducted. The epoxy infiltrated bamboo-composite showed a better ductility toughness of 67.14 kJ/m^2 than the natural bamboo which was at 49.33 kJ/m^2. For the tables comparing epoxy infiltrated bamboo composite with other sources, refer to Tables 1 and 2 in reference (Kalali et al., 2019).

1.4.3 Cellulose fibers reinforcement in ethylene-nonbornene copolymer composite

This study was aimed at making ethylene-norbornene copolymer composites occupied with cellulose fibers and montmorillonite (MMT) (Cichosz, Masek, & Wolski, 2019). The composite was formed and aged to understand any differences that may occur due to it. Furthermore, their structure was investigated to find out their mechanical and optical properties. Additionally, characterization techniques like FTIR have been done. The cellulose fibers were altered with vinyl trimethoxy silane (VTMS) and maleic anhydride (MA) before their surface was made compatible with the polymer matrix improvement using hydrophobization. The employment of natural fibers like cellulose is being sought

after and investigated in resins (Manfredi, Rodríguez, Wladyka-Przybylak, & Vázquez, 2006), thermoplastic (Ruseckaite & Jiménez, 2003), elastomeric materials (Vieira, Nunes, & Visconti, 1996), and in polymer films (Bastos et al., 2016). Natural fibers are currently being used in packaging, automotive, furniture industry, and building constructions (Bachtiar, Sapuan, & Hamdan, 2008).

1.4.3.1 FTIR analysis

An in-depth and accurate analysis of the chemical modifications of treated fibers has been done (Cichosz, Masek, Wolski, & Zaborski, 2019). The analysis exhibited two peaks at 2915 cm^{-1} and another at 2847 cm^{-1} which were accredited to the C-H vibrations and CH_2 groups in the ethylene-norbornene copolymer (Kazayawoko, Balatinecz, & Woodhams, 1997). A band at 1463 cm^{-1} is related to an additional C-H bending of CH_2 (Misra, 1993), another at 718 cm^{-1} was correlated to CH_2 rocking mode. Adsorption bands corresponding to cellulose fibers were found at 1400–800 cm^{-1} (Pandey, 1999). Materials that were treated with cellulose fibers showed bands at concentrations at 1245 cm^{-1} for CH_3 and 1158 cm^{-1} for CO— (Colom, Carrasco, Pages, & Canavate, 2003; Faix, 1991). This proves that the existence of variations in the composite structure was instigated due to the modification of cellulose fibers' presence. The deficiency of —CH_3 and C-O groups provides an intensity surge of other absorption bands that are detected. The usage of VTMS led to the upsurge of absorption band at 1058 cm^{-1} for C-O vibrations (Ołdak, Kaczmarek, Buffeteau, & Sourisseau, 2005). Interestingly, an alteration with MA does not provide any new bands or peaks. These variations in the peak can also be associated with the construction of =C—O—C= bonds (Yang, Zhang, Endo, & Hirotsu, 2003), which may be due to the possibility of cellulose fibers creating new bonds between themselves.

After the aging process, called thermo-oxidizing aging is done; the results of FTIR were again analyzed. For cellulose, the intensity decreases between 1300 and 1100 cm^{-1} due to the drop in the quantity of C-O and —OH entities (Gulmine, Janissek, Heise, & Akcelrud, 2002). An upsurge of intensity is seen at 1100–1000 cm^{-1} which exhibits the existence of CO—O—CO bonds (Fan, Dai, & Huang, 2012) which are in connection with the recombination of C—O bonds inside the composite structure. Another absorption band at 819 cm^{-1} is present for vibrations of C=O and C—O—C groups which were created after the aging procedure was complete. In the case of composites with altered cellulose spectra offered it may be observed that the quantity of C—O, C=O, C=C, and COOH has increased at around 1300–1000 cm^{-1} (Barry, Kamdem, Riedl, & Kaliaguine, 1989; Blackwell, Vasko, & Koenig, 1970) and 830–800 cm^{-1} regions (Santos, Gonzalez, & Gonzalez, 1998). Grafting VTMS and MA with hydroxyl groups on the cellulose surface, changes in the structure of alkyl chains are observed that are bonded to the cellulose fibers, which in turn decreased the signal from —OH entities. This results in a minor modification in the 1700–1500 cm^{-1} region that can be easily observed. This proves the existence of C=C and C=O bonds in the model after aging is done (Hinterstoisser & Salmén, 1999). For the complete table of wave numbers refer to Table 2 of reference (Cichosz, Masek, & Wolski, 2019).

1.4.3.2 Mechanical properties

As reported, tensile properties of composites can be remarkably improved by the addition of fibers to a polymer matrix due to the fact that fibers have better and higher strength and values of stiffness (Holbery & Houston, 2006; Malkapuram, Kumar, & Negi, 2009), but when left unprocessed and natural additives supplemented, composites exhibit inferior tensile strength (Bledzki, Reihmane, & Gassan, 1998) and meagre compatibility with polymer matrix. Here, mechanical properties were analyzed for the determination of standards of the tensile strength (TS) and elongation at breaking (E_b) that is done before and after the aging process, as investigating it was a crucial step for the characterization of composites. Upon investigating the data that were gathered, it was found that mechanical properties changed after the aging process depending upon the orientation of the fibers and were stronger when cellulose or MMT was combined. This proved the point that a controlled aging process was theoretically possible with simple additives like cellulose fibers. The tensile strength before aging was 40 ± 3 MPa and after aging was 37 ± 2 MPa. The percentage of elongation before aging of the composite was at $450 \pm 30\%$ and after aging, the percentage was at around $440 \pm 30\%$. This proved that the degradation process was not intensive, just as the FTIR analysis proved.

1.4.3.3 Optical characterization

Optical properties like the stability of color throughout the aging of the material were inspected to further understand the impact of the aforementioned process. It provides data about the intensity of the various processes performed as the yellowing or browning of samples is a common occurrence which is connected with the aging and can be the evidence of the creation of carbonyl groups in the matrix.

The optical properties of analyzed composites tell that they were affected by the temperatures during the processes. The highest values of color changes were observed for composites occupied with MMT. However, samples made with cellulose and MA-treated natural fibers and MMT mixed with cellulose exhibited color variation at around the same level. Alternatively, VTMS treated with cellulose fibers was the least affected sample due to the aging process, also being the only material changing its optical properties fewer than pure ethylene-norbornene copolymer. On the same page, chroma values associated with saturation were offered. Similarly, this constraint was the most altering and changing in the case of composites treated with MMT. Conversely, changes of chroma values were lowest in the case of the pure ethylene-norbornene copolymer, and the samples present with unchanged or VTMS-treated cellulose, validating its color stability. Saturation was recorded to be the highest in the case of samples treated with MMT and MA natural fibers. It was also observed that VTMS-treated cellulose showed hue angle values wavering between 90° and 100°. This means the color or shade of the samples was similar to yellow. Alternatively, MMT, MA-treated cellulose and cellulose mixed with MMT had angle of hue shifting among 70° and 80° which made their color or shade nearer to orange. Nonetheless, the values of hue angles weren't varying meaningfully after aging producing virtually no

alteration in the shade of the composites. In addition, the authors have a vast experience in the field of nanomaterials and biocomposites (Arpitha, Verma, Sanjay, & Siengchin, 2021; Bharath et al., 2020; Bisht, Verma, Chauhan, & Singh, 2021; Chaudhary, Sharma, & Verma, 2022a, 2022b; Chaurasia, Verma, Parashar, & Mulik, 2019; Deji, Verma, Choudhary, & Sharma, 2021; Deji, Verma, Kaur, Choudhary, & Sharma, 2022; Jain, Verma, & Singh, 2019; Kataria, Verma, Sanjay, & Siengchin, 2022; Rastogi, Verma, & Singh, 2020; Singh, Jain, Verma, Singh, & Chauhan, 2020; Singla, Verma, & Parashar, 2018; Verma et al., 2021; Verma, Baurai, Sanjay, & Siengchin, 2020; Verma, Budiyal, Sanjay, & Siengchin, 2019; Verma, Gaur, & Singh, 2017; Verma, Jain, Kalpana, Siengchin, & Jawaid, 2020; Verma, Jain, Parashar, et al., 2020a, 2020b; Verma, Jain, Rastogi, et al., 2020; Verma, Joshi, Gaur, & Singh, 2018; Verma, Kumar, & Parashar, 2019; Verma, Negi, & Singh, 2018a, 2018b; Verma, Negi, & Singh, 2019; Verma & Parashar, 2017; Verma & Parashar, 2018a; Verma & Parashar, 2018b; Verma & Parashar, 2018c; Verma & Parashar, 2020; Verma, Parashar, Jain, et al., 2020; Verma, Parashar, Singh, et al., 2020; Verma, Parashar, & Packirisamy, 2018a, 2018b; Verma, Parashar, & Packirisamy, 2019a, 2019b; Verma & Singh, 2016; Verma & Singh, 2019; Verma, Singh, & Arif, 2016; Verma, Singh, Singh, & Jain, 2019; Verma, Singh, Verma, & Sharma, 2016; Verma, Zhang, & Van Duin, 2021).

Acknowledgment

Monetary and academic support from the University of Petroleum and Energy Studies, Dehradun, India (SEED Grant program) is highly appreciable.

Conflicts of interest

There are no conflicts of interest to declare by the authors.

References

Abidi, N., Cabrales, L., & Hequet, E. (2010). Thermogravimetric analysis of developing cotton fibers. *Thermochimica Acta*, *498*(1–2), 27–32.

Akil, H., Omar, M. F., Mazuki, A. M., Safiee, S. Z. A. M., Ishak, Z. M., & Bakar, A. A. (2011). Kenaf fiber reinforced composites: A review. *Materials and Design*, *32*(8–9), 4107–4121.

Arpitha, G. R., Verma, A., Sanjay, M. R., & Siengchin, S. (2021). Preparation and experimental investigation on mechanical and tribological performance of hemp-glass fiber reinforced laminated composites for lightweight applications. *Advances in Civil Engineering Materials*, *10*(1), 427–439.

Astley, O. M., & Donald, A. M. (2001). A small-angle X-ray scattering study of the effect of hydration on the microstructure of flax fibers. *Biomacromolecules*, *2*(3), 672–680.

Bachtiar, D., Sapuan, S. M., & Hamdan, M. M. (2008). The effect of alkaline treatment on tensile properties of sugar palm fiber reinforced epoxy composites. *Materials & Design*, *29*(7), 1285–1290.

Balaji, A., Karthikeyan, B., & Sundar, R. C. (2014–2015). Bagasse fiber – The future biocomposite material: A review. *International Journal of Chem Tech Research*, *7*(1), 223–233.

Barry, A. O., Kamdem, P. D., Riedl, B., & Kaliaguine, S. C. (1989). Infrared study of grafted CTMP fibers. *Journal of Wood Chemistry and Technology*, *9*(3), 341–364.

Bastos, M. D. S. R., da Silva Laurentino, L., Canuto, K. M., Mendes, L. G., Martins, C. M., Silva, S. M. F., et al. (2016). Physical and mechanical testing of essential oil-embedded cellulose ester films. *Polymer Testing*, *49*, 156–161.

Bharath, K. N., Madhu, P., Gowda, T. G., Verma, A., Sanjay, M. R., & Siengchin, S. (2020). A novel approach for development of printed circuit board from biofiber based composites. *Polymer Composites*, *41*(11), 4550–4558.

Bhatia, A., Gupta, R. K., Bhattacharya, S. N., & Choi, H. J. (2007). Compatibility of biodegradable poly (lactic acid)(PLA) and poly (butylene succinate)(PBS) blends for packaging application. *Korea-Australia Rheology Journal*, *19*(3), 125–131.

Bisht, N., Verma, A., Chauhan, S., & Singh, V. K. (2021). Effect of functionalized silicon carbide nano-particles as additive in cross-linked PVA based composites for vibration damping application. *Journal of Vinyl and Additive Technology*, *27*(4), 920–932.

Blackwell, J., Vasko, P. D., & Koenig, J. L. (1970). Infrared and Raman spectra of the cellulose from the cell wall of Valonia ventricosa. *Journal of Applied Physics*, *41*(11), 4375–4379.

Bledzki, A. K., Reihmane, S. A., & Gassan, J. (1998). Thermoplastics reinforced with wood fillers: A literature review. *Polymer-Plastics Technology and Engineering*, *37*(4), 451–468.

Braga, R. A., & Magalhaes, P. A. A., Jr. (2015). Analysis of the mechanical and thermal properties of jute and glass fiber as reinforcement epoxy hybrid composites. *Materials Science and Engineering: C*, *56*, 269–273.

Cai, Y., Lv, J., & Feng, J. (2013). Spectral characterization of four kinds of biodegradable plastics: poly (lactic acid), poly (butylenes adipate-co-terephthalate), poly (hydroxybutyrate-co-hydroxyvalerate) and poly (butylenes succinate) with FTIR and Raman spectroscopy. *Journal of Polymers and the Environment*, *21*(1), 108–114.

Chaudhary, A., Sharma, S., & Verma, A. (2022a). WEDM machining of heat treated ASSAB'88 tool steel: A comprehensive experimental analysis. *Materials Today: Proceedings*, *50*(Part 5), 946–951.

Chaudhary, A., Sharma, S., & Verma, A. (2022b). Optimization of WEDM process parameters for machining of heat treated ASSAB'88 tool steel using response surface methodology (RSM). *Materials Today: Proceedings*, *50*(Part 5), 917–922.

Chaurasia, A., Verma, A., Parashar, A., & Mulik, R. S. (2019). Experimental and computational studies to analyze the effect of h-BN nanosheets on mechanical behavior of h-BN/polyethylene nanocomposites. *Journal of Physical Chemistry C*, *123*(32), 20059–20070.

Cheng, G., Varanasi, P., Li, C., Liu, H., Melnichenko, Y. B., Simmons, B. A., et al. (2011). Transition of cellulose crystalline structure and surface morphology of biomass as a function of ionic liquid pretreatment and its relation to enzymatic hydrolysis. *Biomacromolecules*, *12*(4), 933–941.

Cichosz, S., Masek, A., & Wolski, K. (2019). Innovative cellulose fibers reinforced ethylene-norbornene copolymer composites of an increased degradation potential. *Polymer Degradation and Stability*, *159*, 174–183.

Cichosz, S., Masek, A., Wolski, K., & Zaborski, M. (2019). Universal approach of cellulose fibers chemical modification result analysis via commonly used techniques. *Polymer Bulletin*, *76*(5), 2147–2162.

Colom, X., Carrasco, F., Pages, P., & Canavate, J. (2003). Effects of different treatments on the interface of HDPE/lignocellulosic fiber composites. *Composites Science and Technology*, *63*(2), 161–169.

Costa, L. L. D., Monteiro, S. N., & Loiola, R. L. (2011). Characterization of tensile tested continuous bamboo stripped fiber-reinforced epoxy composites. In *EPD Congress 2011* (pp. 289–296). Hoboken, NJ, USA: John Wiley & Sons, Inc.

Deji, R., Verma, A., Choudhary, B. C., & Sharma, R. K. (2021). New insights into NO adsorption on alkali metal and transition metal doped graphene nanoribbon surface: A DFT approach. *Journal of Molecular Graphics and Modelling*, *111*, 108109.

Deji, R., Verma, A., Kaur, N., Choudhary, B. C., & Sharma, R. K. (2022). Density functional theory study of carbon monoxide adsorption on transition metal doped armchair graphene nanoribbon. *Materials Today: Proceedings*, *54*(Part 3), 771–776.

Dursun, T., & Soutis, C. (2014). Recent developments in advanced aircraft aluminium alloys. *Materials and Design*, *56*, 862–871.

Faix, O. (1991). Classification of lignins from different botanical origins by FT-IR spectroscopy. *Holzforschung-International Journal of the Biology, Chemistry, Physics and Technology of Wood*, *45*(s1), 21–28.

Fan, M., Dai, D., & Huang, B. (2012). Fourier transform infrared spectroscopy for natural fibers. In *Vol. 3. Fourier transform-materials analysis* (pp. 45–68). Croatia: InTech.

Faruk, O., Bledzki, A. K., Fink, H. P., & Sain, M. (2012). Biocomposites reinforced with natural fibers: 2000–2010. *Progress in Polymer Science*, *37*(11), 1552–1596.

Fidale, L. C., Ruiz, N., Heinze, T., & Seoud, O. A. E. (2008). Cellulose swelling by aprotic and protic solvents: what are the similarities and differences? *Macromolecular Chemistry and Physics*, *209*(12), 1240–1254.

Frommeyer, G., & Brüx, U. (2006). Microstructures and mechanical properties of high-strength Fe-Mn-Al-C light-weight TRIPLEX steels. *Steel Research International*, *77*(9–10), 627–633.

Gauvin, F., Richard, C., & Robert, M. (2018). Modification of bamboo fibers/bio-based epoxy interface by nano-reinforced coatings. *Polymer Composites*, *39*(5), 1534–1542.

Gilbert, R. D., & Kadla, J. F. (1998). Polysaccharides—Cellulose. In *Biopolymers from renewable resources* (pp. 47–95). Berlin, Heidelberg: Springer.

Guerriero, G., Fugelstad, J., & Bulone, V. (2010). What do we really know about cellulose biosynthesis in higher plants? *Journal of Integrative Plant Biology*, *52*(2), 161–175.

Gulmine, J. V., Janissek, P. R., Heise, H. M., & Akcelrud, L. (2002). Polyethylene characterization by FTIR. *Polymer Testing*, *21*(5), 557–563.

Hinterstoisser, B., & Salmén, L. (1999). Two-dimensional step-scan FTIR: A tool to unravel the OH-valency-range of the spectrum of Cellulose I. *Cellulose*, *6*(3), 251–263.

Holbery, J., & Houston, D. (2006). Natural-fiber-reinforced polymer composites in automotive applications. *JOM*, *58*(11), 80–86.

Jacquet, N., Quievy, N., Vanderghem, C., Janas, S., Blecker, C., Wathelet, B., et al. (2011). Influence of steam explosion on the thermal stability of cellulose fibers. *Polymer Degradation and Stability*, *96*(9), 1582–1588.

Jain, N., Verma, A., & Singh, V. K. (2019). Dynamic mechanical analysis and creep-recovery behaviour of polyvinyl alcohol based cross-linked biocomposite reinforced with basalt fiber. *Materials Research Express*, *6*(10), 105373.

Kalali, E. N., Hu, Y., Wang, X., Song, L., & Xing, W. (2019). Highly-aligned cellulose fibers reinforced epoxy composites derived from bulk natural bamboo. *Industrial Crops and Products*, *129*, 434–439.

Kataria, A., Verma, A., Sanjay, M. R., & Siengchin, S. (2022). Molecular modeling of 2D graphene grain boundaries: Mechanical and fracture aspects. *Materials Today: Proceedings*, *52*(Part 5), 2404–2408.

Kazayawoko, M., Balatinecz, J. J., & Woodhams, R. T. (1997). Diffuse reflectance Fourier transform infrared spectra of wood fibers treated with maleated polypropylenes. *Journal of Applied Polymer Science*, *66*(6), 1163–1173.

Keya, K. N., Kona, N. A., Koly, F. A., Maraz, K. M., Islam, M. N., & Khan, R. A. (2019). Natural fiber reinforced polymer composites: History, types, advantages and applications. *Materials Engineering Research*, *1*(2), 69–85.

Khan, Z., Yousif, B. F., & Islam, M. (2017). Fracture behaviour of bamboo fiber-reinforced epoxy composites. *Composites Part B: Engineering*, *116*, 186–199.

Kushwaha, P. K., & Kumar, R. (2010). Effect of silanes on mechanical properties of bamboo fiber-epoxy composites. *Journal of Reinforced Plastics and Composites*, *29*(5), 718–724.

Ma, P., Wang, X., Liu, B., Li, Y., Chen, S., Zhang, Y., et al. (2012). Preparation and foaming extrusion behavior of polylactide acid/polybutylene succinate/montmorillonoid nanocomposite. *Journal of Cellular Plastics*, *48*(2), 191–205.

Malkapuram, R., Kumar, V., & Negi, Y. S. (2009). Recent development in natural fiber-reinforced polypropylene composites. *Journal of Reinforced Plastics and Composites*, *28*(10), 1169–1189.

Manfredi, L. B., Rodríguez, E. S., Wladyka-Przybylak, M., & Vázquez, A. (2006). Thermal degradation and fire resistance of unsaturated polyester, modified acrylic resins and their composites with natural fibers. *Polymer Degradation and Stability*, *91*(2), 255–261.

Martin, A. R., Martins, M. A., da Silva, O. R., & Mattoso, L. H. (2010). Studies on the thermal properties of sisal fiber and its constituents. *Thermochimica Acta*, *506*(1–2), 14–19.

Mathew, A. P., Oksman, K., & Sain, M. (2005). Mechanical properties of biodegradable composites from poly lactic acid (PLA) and microcrystalline cellulose (MCC). *Journal of Applied Polymer Science*, *97*(5), 2014–2025.

May-Pat, A., Valadez-González, A., & Herrera-Franco, P. J. (2013). Effect of fiber surface treatments on the essential work of fracture of HDPE-continuous henequen fiber-reinforced composites. *Polymer Testing*, *32*(6), 1114–1122.

Misra, G. S. (1993). *Introductory polymer chemistry*. New Age International.

Mohammed, L., Ansari, M. N., Pua, G., Jawaid, M., & Islam, M. S. (2015). A review on natural fiber reinforced polymer composite and its applications. *International Journal of Polymer Science*, *2015*, 243947.

Morán, J. I., Alvarez, V. A., Cyras, V. P., & Vázquez, A. (2008). Extraction of cellulose and preparation of nanocellulose from sisal fibers. *Cellulose*, *15*(1), 149–159.

Mulinari, D. R., & Da Silva, M. L. C. (2008). Adsorption of sulphate ions by modification of sugarcane bagasse cellulose. *Carbohydrate Polymer*, *74*, 617–620.

Mulinari, D. R., Voorwald, H. J., Cioffi, M. O., & da Silva, M. L. (2017). Cellulose fiber-reinforced high-density polyethylene composites—Mechanical and thermal properties. *Journal of Composite Materials*, *51*(13), 1807–1815.

Nguong, C. W., Lee, S. N. B., & Sujan, D. (2013). A review on natural fibre reinforced polymer composites. *International Journal of Materials and Metallurgical Engineering*, *7*(1), 52–59.

Nishida, M., Tanaka, T., Miki, T., Ito, T., & Kanayama, K. (2017). Multi-scale instrumental analyses for structural changes in steam-treated bamboo using a combination of several solid-state NMR methods. *Industrial Crops and Products*, *103*, 89–98.

Okubo, K., Fujii, T., & Yamamoto, Y. (2004). Development of bamboo-based polymer composites and their mechanical properties. *Composites Part A: Applied Science and Manufacturing*, *35*(3), 377–383.

Ołdak, D., Kaczmarek, H., Buffeteau, T., & Sourisseau, C. (2005). Photo- and bio-degradation processes in polyethylene, cellulose and their blends studied by ATR-FTIR and Raman spectroscopies. *Journal of Materials Science*, *40*(16), 4189–4198.

Pandey, K. K. (1999). A study of chemical structure of soft and hardwood and wood polymers by FTIR spectroscopy. *Journal of Applied Polymer Science*, *71*(12), 1969–1975.

Rachini, A., Le Troedec, M., Peyratout, C., & Smith, A. (2009). Comparison of the thermal degradation of natural, alkali-treated and silane-treated hemp fibers under air and an inert atmosphere. *Journal of Applied Polymer Science*, *112*(1), 226–234.

Rastogi, S., Verma, A., & Singh, V. K. (2020). Experimental response of nonwoven waste cellulose fabric–reinforced epoxy composites for high toughness and coating applications. *Materials Performance and Characterization*, *9*(1), 151–172.

Ritchie, R. O. (2011). The conflicts between strength and toughness. *Nature Materials*, *10*(11), 817–822.

Ross, P., Mayer, R., & Benziman, M. (1991). Cellulose biosynthesis and function in bacteria. *Microbiology and Molecular Biology Reviews*, *55*(1), 35–58.

Ruseckaite, R. A., & Jiménez, A. (2003). Thermal degradation of mixtures of polycaprolactone with cellulose derivatives. *Polymer Degradation and Stability*, *81*(2), 353–358.

Sadik, T., Pillon, C., Carrot, C., & Ruiz, J. A. R. (2018). Dsc studies on the decomposition of chemical blowing agents based on citric acid and sodium bicarbonate. *Thermochimica Acta*, *659*, 74–81.

Sánchez, M. L., Aperador, W. A., & Capote, G. (2018). Influence of the delignification process on the properties of panels made with Guadua fibers and plant resin. *Industrial Crops and Products*, *125*, 33–40.

Santos, E. A. G. D. L., Gonzalez, M. J. L., & Gonzalez, M. C. (1998). Modification of polypropylene with maleic anhydride: Ultrasonic irradiation effects. *Journal of Applied Polymer Science*, *68*(1), 45–52.

Shanks, R. A. (2014). Chemistry and structure of cellulosic fibers as reinforcements in natural fiber composites. In *Natural fiber composites* (pp. 66–83). Woodhead Publishing.

Singh, K., Jain, N., Verma, A., Singh, V. K., & Chauhan, S. (2020). Functionalized graphite–reinforced cross-linked poly (vinyl alcohol) nanocomposites for vibration isolator application: Morphology, mechanical, and thermal assessment. *Materials Performance and Characterization*, *9*(1), 215–230.

Singla, V., Verma, A., & Parashar, A. (2018). A molecular dynamics based study to estimate the point defects formation energies in graphene containing STW defects. *Materials Research Express*, *6*(1), 015606.

Taj, S., Munawar, M. A., & Khan, S. (2007). Natural fiber-reinforced polymer composites. *Proceedings-Pakistan Academy of Sciences*, *44*(2), 129.

TheFreeDictionary.com. (n.d.). Cellulose fiber. [online] Available from https://encyclopedia2.thefreedictionary.com/cellulose+fiber.

Thwe, M. M., & Liao, K. (2000). Characterization of bamboo-glass fiber reinforced polymer matrix hybrid composite. *Journal of Materials Science Letters*, *19*(20), 1873–1876.

Uddin, N. (Ed.). (2013). *Developments in fiber-reinforced polymer (FRP) composites for civil engineering* Elsevier.

Uddin, N., Abro, A. M., Purdue, J. D., & Vaidya, U. (2013). *Developments in fiber-reinforced polymer (FRP) composites for civil engineering: 13. Thermoplastic composites for bridge structures*. Elsevier Inc. Chapters.

Verma, A., Baurai, K., Sanjay, M. R., & Siengchin, S. (2020). Mechanical, microstructural, and thermal characterization insights of pyrolyzed carbon black from waste tires reinforced epoxy nanocomposites for coating application. *Polymer Composites*, *41*(1), 338–349.

Verma, A., Budiyal, L., Sanjay, M. R., & Siengchin, S. (2019). Processing and characterization analysis of pyrolyzed oil rubber (from waste tires)-epoxy polymer blend composite for lightweight structures and coatings applications. *Polymer Engineering & Science*, *59* (10), 2041–2051.

Verma, A., Gaur, A., & Singh, V. K. (2017). Mechanical properties and microstructure of starch and sisal fiber biocomposite modified with epoxy resin. *Materials Performance and Characterization*, *6*(1), 500–520.

Verma, A., Jain, N., Kalpana, S. M. R., Siengchin, S., & Jawaid, M. (2020). Natural fibers based bio-phenolic composites. In *Phenolic polymers based composite materials* (pp. 153–168). Singapore: Springer Nature (chapter 10).

Verma, A., Jain, N., Parashar, A., Gaur, A., Sanjay, M. R., & Siengchin, S. (2021). Lifecycle assessment of thermoplastic and thermosetting bamboo composites. In *Bamboo fiber composites* (pp. 235–246). Singapore: Springer.

Verma, A., Jain, N., Parashar, A., Singh, V. K., Sanjay, M. R., & Siengchin, S. (2020a). Design and modeling of lightweight polymer composite structures. In *Lightweight polymer composite structures: Design and manufacturing techniques* (pp. 193–224). Boca Raton: Taylor & Francis Group (CRC Press) (chapter 7).

Verma, A., Jain, N., Parashar, A., Singh, V. K., Sanjay, M. R., & Siengchin, S. (2020b). Lightweight graphene composite materials. In *Lightweight polymer composite structures: Design and manufacturing techniques* (pp. 1–20). Boca Raton: Taylor & Francis Group (CRC Press) (chapter 1).

Verma, A., Jain, N., Rastogi, S., Dogra, V., Sanjay, M. R., Siengchin, S., et al. (2020). Mechanism, anti-corrosion protection and components of anti-corrosion polymer coatings. In *Polymer coatings: Technologies and applications* (pp. 53–66). Boca Raton: Taylor & Francis Group (CRC Press) (chapter 4).

Verma, A., Joshi, K., Gaur, A., & Singh, V. K. (2018). Starch-jute fiber hybrid biocomposite modified with an epoxy resin coating: Fabrication and experimental characterization. *Journal of the Mechanical Behavior of Materials*, *27*(5–6), 1–16.

Verma, A., Kumar, R., & Parashar, A. (2019). Enhanced thermal transport across a bi-crystalline graphene–polymer interface: An atomistic approach. *Physical Chemistry Chemical Physics*, *21*(11), 6229–6237.

Verma, A., Negi, P., & Singh, V. K. (2018a). Physical and thermal characterization of chicken feather fiber and crumb rubber reformed epoxy resin hybrid composite. *Advances in Civil Engineering Materials*, *7*(1), 538–557.

Verma, A., Negi, P., & Singh, V. K. (2018b). Experimental investigation of chicken feather fiber and crumb rubber reformed epoxy resin hybrid composite: Mechanical and microstructural characterization. *Journal of the Mechanical Behavior of Materials*, *27*(3–4), 1–24.

Verma, A., Negi, P., & Singh, V. K. (2019). Experimental analysis on carbon residuum transformed epoxy resin: Chicken feather fiber hybrid composite. *Polymer Composites*, *40*(7), 2690–2699.

Verma, A., & Parashar, A. (2017). The effect of STW defects on the mechanical properties and fracture toughness of pristine and hydrogenated graphene. *Physical Chemistry Chemical Physics*, *19*(24), 16023–16037.

Verma, A., & Parashar, A. (2018a). Molecular dynamics based simulations to study failure morphology of hydroxyl and epoxide functionalised graphene. *Computational Materials Science*, *143*, 15–26.

Verma, A., & Parashar, A. (2018b). Structural and chemical insights into thermal transport for strained functionalised graphene: A molecular dynamics study. *Materials Research Express*, *5*(11), 115605.

Verma, A., & Parashar, A. (2018c). Molecular dynamics based simulations to study the fracture strength of monolayer graphene oxide. *Nanotechnology*, *29*(11), 115706.

Verma, A., & Parashar, A. (2020). Characterization of 2D nanomaterials for energy storage. In *Recent advances in theoretical, applied, computational and experimental mechanics* (pp. 221–226). Singapore: Springer.

Verma, A., Parashar, A., Jain, N., Singh, V. K., Rangappa, S. M., & Siengchin, S. (2020). Surface modification techniques for the preparation of different novel biofibers for composites. In *Biofibers and biopolymers for biocomposites* (pp. 1–34). Cham: Springer.

Verma, A., Parashar, A., & Packirisamy, M. (2018a). Atomistic modeling of graphene/hexagonal boron nitride polymer nanocomposites: A review. *Wiley Interdisciplinary Reviews: Computational Molecular Science*, *8*(3), e1346.

Verma, A., Parashar, A., & Packirisamy, M. (2018b). Tailoring the failure morphology of 2D bicrystalline graphene oxide. *Journal of Applied Physics*, *124*(1), 015102.

Verma, A., Parashar, A., & Packirisamy, M. (2019a). Effect of grain boundaries on the interfacial behaviour of graphene-polyethylene nanocomposite. *Applied Surface Science*, *470*, 1085–1092.

Verma, A., Parashar, A., & Packirisamy, M. (2019b). Role of chemical adatoms in fracture mechanics of graphene nanolayer. *Materials Today: Proceedings*, *11*, 920–924.

Verma, A., Parashar, A., Singh, S. K., Jain, N., Sanjay, M. R., & Siengchin, S. (2020). Modeling and simulation in polymer coatings. In *Polymer coatings: Technologies and applications* (pp. 309–324). Boca Raton: Taylor & Francis Group (CRC Press) (chapter 16).

Verma, A., & Singh, V. K. (2016). Experimental investigations on thermal properties of coconut shell particles in DAP solution for use in green composite applications. *Journal of Materials Science and Engineering*, *5*(3), 1000242.

Verma, A., & Singh, V. K. (2019). Mechanical, microstructural and thermal characterization of epoxy-based human hair–reinforced composites. *Journal of Testing and Evaluation*, *47*(2), 1193–1215.

Verma, A., Singh, V. K., & Arif, M. (2016). Study of flame retardant and mechanical properties of coconut shell particles filled composite. *Research and Reviews: Journal of Material Sciences*, *4*(3), 1–5.

Verma, A., Singh, C., Singh, V. K., & Jain, N. (2019). Fabrication and characterization of chitosan-coated sisal fiber – Phytagel modified soy protein-based green composite. *Journal of Composite Materials*, *53*(18), 2481–2504.

Verma, A., Singh, V. K., Verma, S. K., & Sharma, A. (2016). Human hair: A biodegradable composite fiber—A review. *International Journal of Waste Resources*, *6*(206), 2.

Verma, A., Zhang, W., & Van Duin, A. C. (2021). ReaxFF reactive molecular dynamics simulations to study the interfacial dynamics between defective h-BN nanosheets and water nanodroplets. *Physical Chemistry Chemical Physics*, *23*(18), 10822–10834.

Vieira, A., Nunes, R. C., & Visconti, L. L. (1996). Mechanical properties of NR/BR/cellulose II composites. *Polymer Bulletin*, *36*(6), 759–766.

Vorawongsagul, S., Pratumpong, P., & Pechyen, C. (2021). Preparation and foaming behavior of poly (lactic acid)/poly (butylene succinate)/cellulose fiber composite for hot cups packaging application. *Food Packaging and Shelf Life*, *27*, 100608.

Wang, K., Jiao, T., Wang, Y., Li, M., Li, Q., & Shen, C. (2013). The microstructures of extrusion cast biodegradable poly (butylene succinate) films investigated by X-ray diffraction. *Materials Letters*, *92*, 334–337.

Yang, K., Wu, S. J., Guan, J., Shao, Z. Z., & Ritchie, R. O. (2017). Enhancing the mechanical toughness of epoxy-resin composites using natural silk reinforcements. *Scientific Reports*, *7*, 11939.

Yang, L., Zhang, F., Endo, T., & Hirotsu, T. (2003). Microstructure of maleic anhydride grafted polyethylene by high-resolution solution-state NMR and FTIR spectroscopy. *Macromolecules*, *36*(13), 4709–4718.

Yu, Y., Huang, X., & Yu, W. (2014). A novel process to improve yield and mechanical performance of bamboo fiber-reinforced composite via mechanical treatments. *Composites Part B: Engineering*, *56*, 48–53.

Yu, P., Mi, H. Y., Huang, A., Geng, L. H., Chen, B. Y., Kuang, T. R., et al. (2015). Effect of poly (butylenes succinate) on poly (lactic acid) foaming behavior: Formation of open cell structure. *Industrial & Engineering Chemistry Research*, *54*(23), 6199–6207.

Zhang, Y., Hou, Q., Xu, W., Qin, M., Fu, Y., Wang, Z., et al. (2017). Revealing the structure of bamboo lignin obtained by formic acid delignification at different pressure levels. *Industrial Crops and Products*, *108*, 864–871.

Zhang, Y., Qin, M., Xu, W., Fu, Y., Wang, Z., Li, Z., et al. (2018). Structural changes of bamboo-derived lignin in an integrated process of autohydrolysis and formic acid inducing rapid delignification. *Industrial Crops and Products*, *115*, 194–201.

Zhao, H., Kwak, J. H., Zhang, Z. C., Brown, H. M., Arey, B. W., & Holladay, J. E. (2007). Studying cellulose fiber structure by SEM, XRD, NMR and acid hydrolysis. *Carbohydrate Polymers*, *68*(2), 235–241.

Zini, E., & Scandola, M. (2011). Green composites: An overview. *Polymer Composites*, *32*(12), 1905–1915.